Journal of
**Applied Crystallography**

ISSN 0021-8898

Received 8 January 2013
Accepted 28 February 2013

# Using a non-monochromatic microbeam for serial snapshot crystallography

**Catherine Dejoie,[a,b]* Lynne B. McCusker,[a] Christian Baerlocher,[a] Rafael Abela,[b] Bruce D. Patterson,[b] Martin Kunz[c] and Nobumichi Tamura[c]**

[a]Laboratory of Crystallography, ETH Zurich, Wolfgang-Pauli-Strasse 10, Zurich CH-8093, Switzerland, [b]Paul Scherrer Institut, Villigen PSI, 5232, Switzerland, and [c]Advanced Light Source, Lawrence Berkeley National Laboratory, 1 Cyclotron Road, Berkeley, CA 94720, USA. Correspondence e-mail: c.dejoie@mat.ethz.ch, cdejoielbl@gmail.com

The new X-ray free-electron laser source (SwissFEL) that is currently being developed at PSI will provide a broad-bandpass mode with an energy bandwidth of about 4%. By using the full energy range, a new option for structural studies of crystalline materials may become possible. The proof of concept of broad-bandpass diffraction presented here is based on Laue single-crystal microdiffraction and the experimental setup on BL12.3.2 at the Advanced Light Source in Berkeley. Diffraction patterns for 100 randomly oriented stationary crystallites of the **MFI**-type zeolite ZSM-5 were simulated assuming several bandwidths, and the statistical and structural results are discussed. With a 4% energy bandwidth, the number of reflection intensities measured in a single shot is significantly higher than with monochromatic radiation. Furthermore, the problem of partial reflection measurement, which is inherent to the monochromatic mode with stationary crystals, can be overcome.



## 1. Introduction

New X-ray free-electron laser (XFEL) sources that create X-ray pulses of unprecedented brilliance open up new possibilities for the structural characterization of crystalline materials. By exposing small crystallites (from nano- to a few micrometres in size) to a single ultrafast pulse, a diffraction pattern can be obtained before the crystal is damaged. By combining such single-pulse diffraction patterns collected sequentially on many randomly oriented crystallites, it should be possible to avoid radiation damage effects and to determine the structure of the material accurately. Emerging techniques such as serial femtosecond crystallography (Chapman *et al.*, 2011) have recently been applied successfully to the structural characterization of small protein crystals (Boutet *et al.*, 2012; Johansson *et al.*, 2012; Koopman, 2012). This method requires the collection of a huge number of monochromatic single-crystal X-ray diffraction patterns from randomly oriented crystals. One of the drawbacks of this approach is that only a single position of the Ewald sphere is accessed in each pattern, so, because reflections have a finite width, the diffraction condition is not satisfied completely for any of the reflections recorded. Consequently, a Monte Carlo method has to be applied to retrieve interpretable intensities (Kirian *et al.*, 2011).

A new XFEL source (SwissFEL) is currently being developed at PSI (Patterson *et al.*, 2010), and a broad-bandpass mode with an energy spread of about 4% is planned. The use of such an 'extra pink' beam in a diffraction experiment with stationary crystallites should not only increase the number of reflection intensities that can be collected in a single shot, but also overcome the problem of 'partial reflection' measurement that is inherent to the monochromatic experiment. We propose a new approach inspired by both monochromatic single-crystal diffraction and Laue single-crystal (micro)-diffraction. As in the serial femtosecond crystallography approach, many patterns need to be collected sequentially on randomly oriented microcrystals. However, the broad-bandpass beam should allow the number of patterns required to be reduced significantly.

Methodology for structure determination using Laue diffraction was first developed at the end of the 1980s for the protein community (Helliwell, Habash *et al.*, 1989). However, only a few applications to small-molecule and/or inorganic structures have been reported (Harding *et al.*, 1988; Gomez de Anderez *et al.*, 1989). The sensitivity of the Laue method for the quantitative analysis of small-molecule or protein structures was demonstrated most convincingly with the location of hydrogen atoms and water molecules from difference Fourier maps generated using such data (Helliwell, Gomez de Anderez *et al.*, 1989; Lindahl *et al.*, 1992). The technique has also been applied very successfully in the past decade to map grain orientation and crystal distortion in polycrystalline and composite materials with a spatial resolution from a few micrometres to the submicrometre scale (Tamura *et al.*, 2003; Chen *et al.*, 2011).

In the proof-of-concept study described here, diffraction patterns for 100 randomly oriented **MFI**-type zeolite crystals were simulated assuming several energy bandwidth values. The first step in data processing involves indexing each of the large number of diffraction patterns. This and subsequent data analysis were performed using a Laue microdiffraction approach.

## 2. Strategy

A Laue microdiffraction experiment was conducted on Beamline 12.3.2 at the Advanced Light Source (ALS) of Lawrence Berkeley National Laboratory. This beamline is characterized by an energy range of 5–24 keV and a beam size of 1 × 1 µm. Crystals of the zeolite ZSM-5 (**MFI** type, *Pnma*, $a$ = 20.022, $b$ = 19.899, $c$ = 13.383 Å; van Koningsveld *et al.*, 1987) were randomly dispersed on a glass slide.

**Table 1**
Completeness results obtained with the first two-dimensional detector configuration (DET1, 100 crystal orientations), with the second detector configuration (DET2, 100 crystal orientations), and by combining both setups (DET1 + DET2, 200 crystal orientations) at 4% bandwidth value.

| | Total No. of reflections | Full resolution range (Å) | No. of unique reflections | Completeness (%) | Shorter resolution range (Å) | No. of unique reflections | Completeness (%) |
|---|---|---|---|---|---|---|---|
| DET1 | 14054 | 0.654–1.351 | 6039 | 66 | 1.0–2.5 | 4720 | 71 |
| DET2 | 4601 | 0.936–8.016 | 2278 | 65 | 0.7–1.2 | 1974 | 73 |
| DET1 + DET2 | 18655 | 0.654–8.016 | 7428 | 73 | 0.9–2.5 | 3036 | 81 |

This glass slide was then placed at 45° relative to the incident X-ray beam, and Laue diffraction patterns were collected in reflection geometry using a two-dimensional Pilatus 1M detector (Henrich *et al.*, 2009) mounted perpendicular to the incident beam. More details on the experimental setup are described by Kunz *et al.* (2009). One hundred Laue diffraction patterns were collected on different crystallites on the slide and indexed using the software package *XMAS* (Tamura *et al.*, 2003).

Orientation matrices from these measurements were then used to simulate broad-bandpass diffraction patterns in the relevant energy range for two different detector setups using a transmission geometry (Fig. 1). In the first setup, the detector was positioned at 90° 2$\theta$ (DET1). With this setup, more reflections are collected in one shot, because they are concentrated on the higher-resolution range ($d$ values between 0.65 and 1.36 Å). In the second setup, the two-dimensional detector was positioned at 45° 2$\theta$ (DET2). In this case, the detector position was chosen as a compromise between quantity of data (high 2$\theta$ values as in the first setup) and access to low-resolution data at low 2$\theta$ angle (detector at 0°). For both setups, the sample holder was oriented at 45° relative to the incoming beam and the distance from the sample to the center of the detector was kept at 140 mm. A nominal energy of 12 keV was chosen to reflect the expected characteristics of the SwissFEL beam. Simulations were performed from 0.5 to 5% bandwidths using the *XMAS* software. All simulations were thus based on crystallite orientations that had been measured in a real experiment and experimental setups already established on ALS BL12.3.2. The Ewald construction for Laue mode (5–24 keV), 4% bandwidth 'extra pink' beam mode and monochromatic mode is shown in Fig. 2.

The broad-bandpass simulated diffraction patterns were indexed using a pattern recognition algorithm based on the one described by Van Wamelen *et al.* (2004) and recently implemented in the *XMAS* software. This algorithm proved to be efficient for indexing data sets obtained in the 5–2% bandwidth range. Some preliminary tests were also carried out on diffraction patterns simulated for several grains diffracting simultaneously in a single shot. The indexing seemed to be successful for up to two or three orientations at a time for bandwidths greater than 3.5%.

## 3. Statistics

The total number of reflections and the number of unique reflections obtained by combining the data from all 100 crystal orientations for both experimental setups (DET1 and DET2) are plotted in Fig. 3(*a*). Completeness (number of unique reflections simulated *versus* total number present in the corresponding resolution range) results are given in Fig. 3(*b*). As expected, the total number of reflections for each bandwidth value is higher with DET1 (resolution range 0.654–1.351 Å) than with DET2 (resolution range 0.936–8.016 Å). As might be expected, the number of simulated reflections for both setups

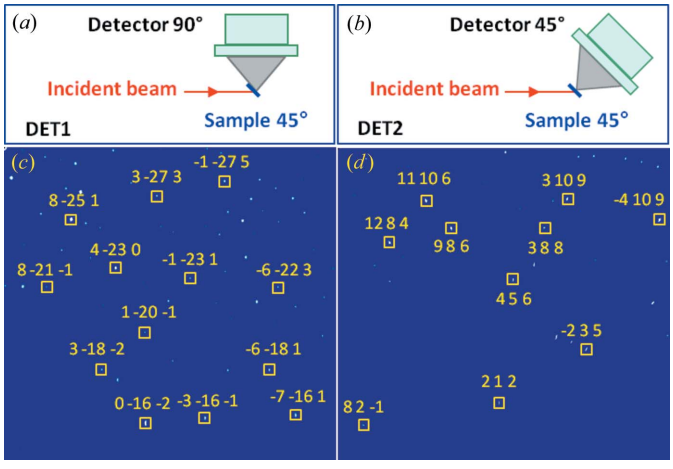


**Figure 1**
(*a*) Experimental setup with the two-dimensional detector at 90° relative to the incoming beam (DET1). (*b*) Experimental setup with the two-dimensional detector at 45° relative to the incident beam (DET2). (*c*) Simulated pattern obtained with DET1 with a 4% energy bandwidth centered at 12 keV. The indexing of some peaks is shown. (*d*) Simulated pattern obtained with DET2 with a 4% energy bandwidth.

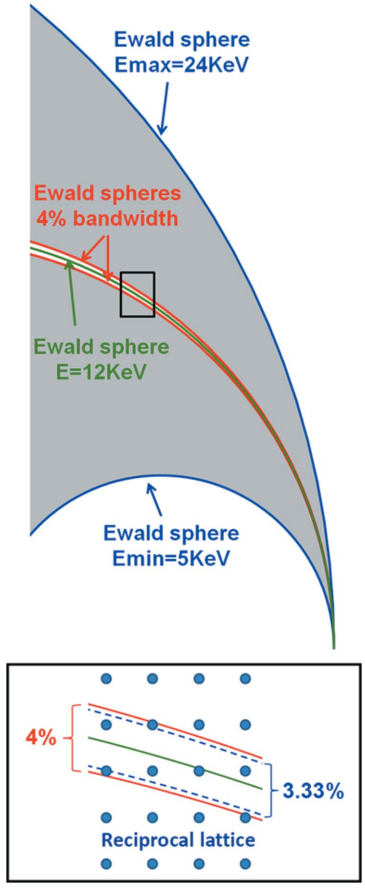


**Figure 2**
Ewald construction for Laue mode (5–24 keV), monochromatic mode (12 keV) and 4% bandwidth 'extra pink' beam mode. The inset shows that the partial reflection intensity problem can be overcome when using a non-monochromatic beam.

**Table 2**
Structure solution results (XD = dual-space method, XS = direct methods) using data sets obtained with DET1, with DET2 and by combining the two (DET1 + DET2).

The structure is considered to be solved when at least 10 of the 12 Si atoms in the asymmetric unit are found.

| Bandwidth (%) | 1 | 2 | 3 | 4 | 5 |
|---|---|---|---|---|---|
| DET1 | XD | XD | XD | XD | XD |
| DET2 | – | – | XD | XD | XD/XS |
| DET1 + DET2 | XD | XD | XD/XS | XD/XS | XD/XS |

increases linearly with bandwidth. Results obtained for a 4% bandwidth are summarized in Table 1. With this bandwidth, 14 054 reflections, of which 6039 are unique, are simulated for DET1 and 4601 reflections, of which 2278 are unique, for DET2. On average, there are 140 reflections per pattern with DET1 and 46 reflections with DET2. A completeness value of *ca* 65% was calculated in both cases for the respective resolution ranges. By reducing the resolution range to 0.7–1.2 Å with DET1 and to 1.0–2.5 Å with DET2, the completeness increases to 71 and 73%, respectively. This is because the number of simulated reflections near the lower limits of the resolution ranges is a smaller fraction of the possible reflections in this range.

The two data sets obtained with DET1 and DET2 were then combined to simulate an experimental setup in which two detectors are used simultaneously. Completeness calculation results are shown in Fig. 3(*b*). With a 4% bandwidth, completeness values of 73 and 81% are obtained for the full resolution range (0.654–8.016 Å) and the reduced range (0.9–2.5 Å), respectively. This is a gain of 7–10% compared with the single-detector setup. Increasing the number of combined crystal orientations would, of course, increase the completeness. However, these simulations are based on real data taken from crystals dispersed on a glass slide. The crystals exhibit a 'coffin-like' morphology, so it is expected that some orientations will be very rare or absent, and this will lead to an upper limit on the completeness that is less than 100%, as indicated in Fig. 3(*b*).

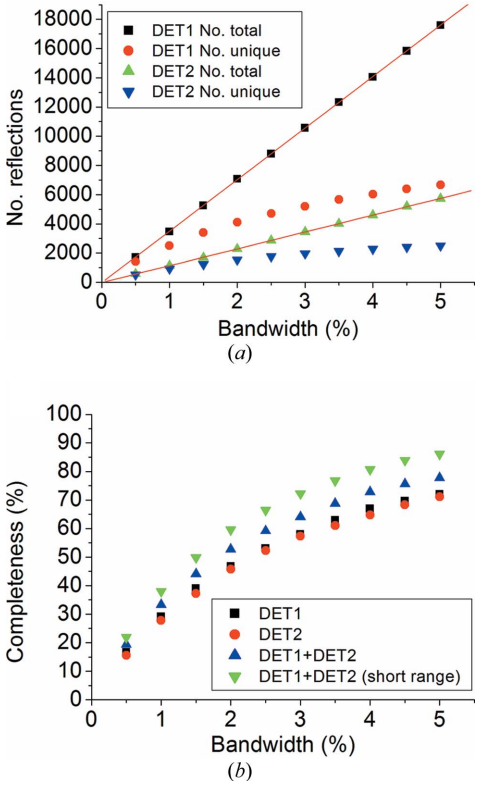


**Figure 3**
(*a*) Total number of reflections and number of unique reflections simulated by combining the data from 100 orientations, as a function of the energy bandwidth. The total number of reflections in both cases increases linearly. (*b*) Completeness results as a function of the energy bandwidth, obtained by combining the data from 100 orientations with DET1 (resolution range 0.654–1.351 Å) and with DET2 (resolution range 0.936–8.016 Å), and by combining the data from both setups (DET1 + DET2: resolution range 0.654–8.016 Å; DET1 + DET2 (short range): resolution range 0.9–2.5 Å).

Structure solution using only the reflections that could be accessed according to the simulations was carried out with the *SHELX* software (Sheldrick, 2008). Both direct (*SHELXS*) and dual-space (*SHELXD*) methods were tested. The results obtained are summarized in Table 2. With data sets obtained separately with DET1 or DET2, direct methods failed most of the time. This result is attributed to the fact that most of the low-resolution data are missing with DET1, and the number of data is not sufficient with DET2 (except for a 5% bandwidth). However, the structure could be solved using the dual-space approach for bandwidth values higher than 1 and 3% with DET1 and DET2, respectively. By combining the data from both detector positions (DET1 + DET2), structure solution was successful using both dual-space and direct methods for bandwidth values higher than 3%.

## 4. Partial reflection measurement

In order to calculate whether or not the use of a broad-bandpass beam can help to overcome the partial reflection measurement problem, the width in energy of the reflections from the sample of interest has to be known. This width will, of course, depend on the mosaicity of the sample and some parameters of the X-ray source. In the experiment performed at ALS, the width in energy of 18 reflections was measured over the 8–16 keV range for the ZSM-5 sample by performing an energy scan with a monochromatic beam. Data were collected on three different crystals. The energy scan of one reflection centered at 7.987 keV is shown in Fig. 4. The energy widths of all 18 reflections were found to lie between 40 and 80 eV. Thus, to measure the intensity of a reflection of this ZSM-5 sample completely, the energy center of a reflection must, in the worst case, be at least 40 eV away from the low-energy and high-energy cutoffs. For a 12 keV beam, this represents 0.33% bandwidth, so the total bandwidth has to be reduced by 0.66%. By using a 4% bandwidth 'extra pink' beam centered at 12 keV, we can expect that all reflections within the energy range of a 3.33% bandwidth will be correctly measured (Fig. 2).

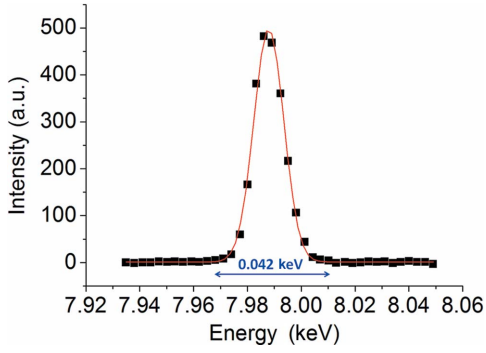


**Figure 4**
Energy scan with a monochromatic beam for the 1 $\overline{13}$ 3 reflection of a ZSM-5 crystal. The profile fit was used to extract the energy width of the reflection.

With the data from both detector positions (DET1 + DET2) and a 4% bandwidth, the reflection redundancy is 2.5. Even if a higher redundancy is necessary for real data, the very high redundancy required in XFEL experiments with a monochromatic beam will not be required, because the partial intensity measurement can be avoided.

## 5. Conclusion

The potential benefits of using a non-monochromatic broad-bandpass beam to collect single-crystal data from randomly oriented microcrystals have been demonstrated. By using a beam with a 4% energy bandwidth, the number of accessible reflections that are not affected by the partial reflection intensity problem increases significantly. The number of data collected in a single shot could be increased further by using several detectors and by exposing several crystals to the beam simultaneously. The next step will be to apply the method to real data, in order to tackle the problems of intensity corrections and scaling. Our prime interest is in the area of inorganic and small-molecule structures, where the diffraction patterns are sparse, but this new approach could also be of benefit to the protein community. The 'extra pink' beam mode option offers a clear opportunity to ease the data acquisition in femtosecond time-resolved experiments at an XFEL facility. This could be of particular importance in studies of irreversible processes, a challenging problem identified by Nieh *et al.* (1999). The method requires a beam with a few per cent energy bandwidth, so it could also be of interest for the new compact light sources such as LCS Lyncean (Bech *et al.*, 2009) and ThomX (Variola, 2011), and for synchrotron facilities, where appropriate bandwidths might be generated by undulators (Plech *et al.*, 2002).

CD is supported by Chevron (Richmond, CA, USA) and PSI (Villigen, CH). The Advanced Light Source at the Lawrence Berkeley National Laboratory is supported by the Office of Science, Office of Basic Energy Sciences, Scientific User Facilities Division of the US Department of Energy under contract No. DE-AC02-05CH11231.

## References

Bech, M., Bunk, O., David, C., Ruth, R., Rifkin, J., Loewen, R., Feidenhans'l, R. & Pfeiffer, F. (2009). *J. Synchrotron Rad.* **16**, 43–47.
Boutet, S. *et al.* (2012). *Science*, **337**, 362–364.
Chapman, H. N. *et al.* (2011). *Nature*, **470**, 73–77.
Chen, K., Kunz, M., Tamura, N. & Wenk, H. (2011). *Phys. Chem. Miner.* **38**, 491–500.
Gomez de Anderez, D., Helliwell, M., Habash, J., Dodson, E. J., Helliwell, J. R., Bailey, P. D. & Gammon, R. E. (1989). *Acta Cryst.* B**45**, 482–488.
Harding, M. M., Maginn, S. J., Campbell, J. W., Clifton, I. & Machin, P. (1988). *Acta Cryst.* B**44**, 142–146.
Helliwell, M., Gomez de Anderez, D., Habash, J., Helliwell, J. R. & Vernon, J. (1989). *Acta Cryst.* B**45**, 591–596.
Helliwell, J. R., Habash, J., Cruickshank, D. W. J., Harding, M. M., Greenhough, T. J., Campbell, J. W., Clifton, I. J., Elder, M., Machin, P. A., Papiz, M. Z. & Zurek, S. (1989). *J. Appl. Cryst.* **22**, 483–497.
Henrich, B., Bergamaschi, A., Broennimann, C., Dinapoli, R., Eikenberry, E., Johnson, I., Kobas, M., Kraft, P., Mozzanica, A. & Schmitt, B. (2009). *NIMA*, **607**, 247–249.
Johansson, L. C. *et al.* (2012). *Nat. Methods*, **9**, 263–265.
Kirian, R. A., White, T. A., Holton, J. M., Chapman, H. N., Fromme, P., Barty, A., Lomb, L., Aquila, A., Maia, F. R. N. C., Martin, A. V., Fromme, R., Wang, X., Hunter, M. S., Schmidt, K. E. & Spence, J. C. H. (2011). *Acta Cryst.* A**67**, 131–140.
Koningsveld, H. van, van Bekkum, H. & Jansen, J. C. (1987). *Acta Cryst.* B**43**, 127–132.
Koopman, R. *et al.* (2012). *Nat. Methods*, **9**, 259–262.
Kunz, M. *et al.* (2009). *Rev. Sci. Instrum.* **80**, 035108.
Lindahl, M., Liljas, A., Habash, J., Harrop, S. & Helliwell, J. R. (1992). *Acta Cryst.* B**48**, 281–285.
Nieh, Y. P., Raftery, J., Weisgerber, S., Habash, J., Schotte, F., Ursby, T., Wulff, M., Hädener, A., Campbell, J. W., Hao, Q. & Helliwell, J. R. (1999). *J. Synchrotron Rad.* **6**, 995–1006.
Patterson, B. D. *et al.* (2010). *New J. Phys.* **12**, 035012.
Plech, A., Randler, R., Geis, A. & Wulff, M. (2002). *J. Synchrotron Rad.* **9**, 287–292.
Sheldrick, G. M. (2008). *Acta Cryst.* A**64**, 112–122.
Tamura, N., MacDowell, A. A., Spolenak, R., Valek, B. C., Bravman, J. C., Brown, W. L., Celestre, R. S., Padmore, H. A., Batterman, B. W. & Patel, J. R. (2003). *J. Synchrotron Rad.* **10**, 137–143.
Van Wamelen, P., Li, Z. & Iyengar, S. (2004). *Pattern Recognit.* **37**, 1699–1711.
Variola, A. (2011). *Proceedings of IPAC2011, San Sebastian, Spain. Synchrotron Light Sources and FELs, Advanced Concepts*, pp. 1903–1905, http://accelconf.web.cern.ch/accelconf/IPAC2011/papers/weoaa01.pdf.